



## Original article

Molecules and functions of rosewood: *Pterocarpus santalinus*Shuaicheng Jiang<sup>a,b</sup>, Yanqiang Wei<sup>b</sup>, Zhenling Liu<sup>c</sup>, Changyu Ni<sup>b</sup>, Haiping Gu<sup>a</sup>, Wanxi Peng<sup>a,b</sup><sup>a</sup> Henan Province Engineering Research Center for Forest Biomass Value-added Products, Henan Agricultural University, Zhengzhou 450002, China<sup>b</sup> College of Materials Science and Engineering, Central South University of Forestry and Technology, Changsha 410004, China<sup>c</sup> School of Management, Henan University of Technology, Zhengzhou 450001, China

## ARTICLE INFO

## Article history:

Received 22 September 2019

Revised 17 December 2019

Accepted 1 January 2020

Available online 10 January 2020

## Keywords:

*Pterocarpus santalinus*

Chemical composition

Extract

Redwood

GC–MS

## ABSTRACT

People raise redwood, and mahogany will last a lifetime. In China, there have always been the sayings of “sleeping *Pterocarpus indicus* Willd. and sitting on *Dalbergia cochinchinensi*”. Among them, the health of mahogany furniture is rarely scientifically and systematically elaborated. Therefore, the active ingredients in the *Pterocarpus santalinus* extract were analyzed in detail by using advanced detection techniques, and it was found that 54 active ingredients were detected in the *Pterocarpus santalinus* extract. Mainly include alkanes, phenols, alcohols, terpenes (alkenes), and acids. In the *Pterocarpus santalinus* extract, the majority components of *Pterocarpus santalinus* are healthy and abundant; the main representative of the active ingredient were .alpha.-Bisabolol, Squalene, cedrol, Propanoic acid, 2-methyl-, 3-hydroxy-2,2,4-trimethylpentyl ester, P-Cresol, (-) - Spathulenol and Heptacosane. It also has potential application prospects in the fields of bio-energy, bio-medicine, cosmetics, skin care products, and spices. The study of the chemical composition of *Pterocarpus santalinus* provides a scientific basis for the development and utilization of the plant.

© 2020 Published by Elsevier B.V. on behalf of King Saud University. This is an open access article under the CC BY-NC-ND license (<http://creativecommons.org/licenses/by-nc-nd/4.0/>).

## 1. Introduction

*Pterocarpus santalinus* belongs to the butterfly-shaped red sandalwood flowers, classified as rosewood mahogany, are medium arbor, found mainly in India, has deep and white stripes, and is slightly fragrant. Because of the pterocarpin, it is soluble in alcohol and ether; wood chips in the alcohol were orange, and the fingers dipped in alcohol or water and wood friction was red (Anuradha and Pullaiah, 1999; Manjunatha, 2006).

The chemical composition of wood is complex and diverse—mainly consisting of carbohydrates, phenols, terpenes, fatty acids, etc.—which can also be divided into fiber hemicellulose, lignin, and extract (Esteves et al., 2008). The chemical composition of different woods is varied, but the chemical composition of the same wood is usually more fixed. This chemical composition affects the physical mechanics, natural durability, color, smell, and taste

of the wood, as well as its processing and utilization (Esteves and Pereira, 2009; Mohareb et al., 2012). Wood moisture absorption is mainly due to the presence of hydrophilic and free hydroxyl groups on the cellulose (Endo et al., 2016; Peng et al., 2018). Lignin is a kind of complex aromatic substance; the chemical structure of lignin and wood species has an important impact on the color of the wood (Huang et al., 2016; Wang et al., 2015). Experimental results from Zhang Shuangyan et al. (2013) show that the content of lignin and a single fiber elastic modulus positively correlated with a higher cellulose content and fiber tensile strength. Hemicellulose and lignin as a bonding material and hard solid material give the wood elasticity and compressive strength (Esteves et al., 2008; Fidêncio, 2011; Shen et al., 2017). In addition to the three elements, wood also contains certain types and quantities of extracts, such as volatile oils, resins, and other phenolic compounds (Aydemir et al., 2011; Tumen et al., 2010). The wood has a different color, which is associated with the cell cavity, whether the cell wall is filled or deposited extract. Some species contain natural pigments, such as flavonoids and ketones, etc.; the heartwood was red because the redwood heartwood contains redwood pigment, while the mahogany contains magenta hematoxylin pigment, so that redwood was red. Balaban (2004) studied the phenolic compounds of sapwood and heartwood by GC–MS. Arias et al. (2012) also detected and analyzed lignin heat transfer decomposition of the

Peer review under responsibility of King Saud University.



Production and hosting by Elsevier

<https://doi.org/10.1016/j.jksus.2020.01.006>

1018-3647/© 2020 Published by Elsevier B.V. on behalf of King Saud University.

This is an open access article under the CC BY-NC-ND license (<http://creativecommons.org/licenses/by-nc-nd/4.0/>).

material by GC–MS of pyrolysis pine at different high temperatures.

In order to scientifically and systematically explain the mahogany in depth, so that people can have a clearer understanding of the way of redwood health; at the same time, studying the chemical composition of wood can provide a basis for the processing and utilization of wood. Therefore, sandalwood was used as the research object, and the organic solvent extracts were analyzed by advanced detection methods (such as FT-IR, TG, GC–MS, PY–GC–MS, and TDS–GC–MS). The molecular composition of sandalwood extract was deeply analyzed through comparative analysis, and the prospect of resource utilization was prospected (Mi et al., 2019).

## 2. Material and methods

**Extraction methods:** Samples were crushed into 40–60 mesh powder by a crusher. Then, dry 10%, take 10 g (accuracy: 0.1 mg) of dried *Pterocarpus santalinu* sample, put into distillation bottles, add 300 mL (accuracy: 1 mL) of ethanol, ethanol/benzene (1:1), and methanol/ethanol (1:1) solvent was used to extract, respectively. The extraction were named B1, B2, and B3 samples. The mixture of reagents was extracted for 5 h at 85 °C, then the solid powder was named B1-1, B2-2, and B3-3 samples, respectively.

To determine the functional groups and chemical bonding present in the extract of the *Pterocarpus santalinu*, FT-IR analysis was conducted with a FT-IR spectrophotometer (Thermo Fisher Scientific iS100) at 4000–400  $\text{cm}^{-1}$ . FT-IR test sample was prepared by mixing the sample with KBr in a ratio of 1:100. The instrument records infrared molecular absorption, infrared spectrum acquisition, spectral smoothing and baseline correction. Infrared spectroscopy usually takes wave ( $\sigma$ ) as abscissa to indicate the position of absorption peak, and vertical axis transmittance to indicate absorption intensity (Jiang et al., 2017; Peng et al., 2014; Xue et al., 2014).

The chemical components present in the samples were determined by a GC–MS (Agilent 7890B-5977A). The column used was elastic quartz capillary column named HP-5MS (30 m  $\times$  250  $\mu\text{m}$   $\times$  0.25  $\mu\text{m}$ ). High purity helium (1 mL/min) was used as the carrier gas and the split ratio was 2:1. The GC oven was started at 50 °C, and heated to 250 °C (ramping rate = 8 °C/min), and then further heated up to 280 °C (ramping rate = 5 °C/min). For the MS, compounds in the mass range of 30–600 amu were detected. Meanwhile, the ionization voltage and current were 70 eV and 150  $\mu\text{A}$  EI, respectively. The quadrupole and the ion source temperature were set at 150 °C and 230 °C, respectively.

Fast pyrolysis of *Pterocarpus santalinu* were performed and analyzed via thermogravimetry (TG), and pyrolysis/GC–MS (Py/GC–MS). The performance of the four samples were investigated and compared. The thermogravimetric analyzer (TGA) is used to study the thermal stability and composition of materials. For TG analysis, 4–7 mg of the samples were analyzed using TGA Q50 V20.8 Build 34. Instruments to determine the thermal decomposition of the samples. The sample was from 30 °C to 250 °C under nitrogen flow (60 mL/min) with two different ramping rates of 5 °C/min. Py/GC–MS (CDS5200-trace1310 ISQ) equipped with TR-5MS capillary column (30 m  $\times$  0.25 mm  $\times$  0.25  $\mu\text{m}$ ) was used during Py/GC–MS test. The sample was from 30 °C to 500 °C (ramping rate = 20 °C/ms) under inert helium flow (50 mL/min) for 15 s, before the product sample was subjected to GC. The GC was operated under split mode with split ratio of 60:1. The GC oven was started at 40 °C (holding time = 2 min), heated to 120 °C (ramping rate = 5 °C/min), and then further increased to 200 °C (ramping rate = 10 °C/min, holding time = 15 min). For the MS, the ion source [electron ionization (EI)] temperature and scanning range were set at 280 °C and

28–500 amu. TD/GC–MS: First, the sample was from 30 °C to 100 °C (ramping rate = 10 °C/min, retained for 5 min), then 100 °C–200 °C (ramping rate = 10 °C/min, retained for 0 min) (Peng et al., 2012).

## 3. Results and discussion

### 3.1. Analysis of FT-IR

The infrared spectrum of *Pterocarpus santalinus* was analyzed. Fig. 1 shows the infrared contrast spectra of the *Pterocarpus santalinus* and the three extracts. The absorption peak in infrared spectrum is the stretching vibration of free hydroxyl above 3400  $\text{cm}^{-1}$ . The broad peak is an intermolecular association absorption peak near 3400  $\text{cm}^{-1}$ . The absorption peak is the stretching vibration of the saturated C–H bond at 3000–2750  $\text{cm}^{-1}$ . The absorption peak at 1800–1580  $\text{cm}^{-1}$  was attributed to the C=O stretching vibration. The absorption peak at 1480–1300  $\text{cm}^{-1}$  is mostly  $\text{CH}_2$  and  $\text{CH}_3$  bending vibration absorption. The absorption peaks near 1450  $\text{cm}^{-1}$  and 1350  $\text{cm}^{-1}$  are  $\text{CH}_2$  stretching vibration and  $\text{CH}_3$  stretching vibration, respectively. The absorption peak is mainly caused by C–C stretching vibration, C–O stretching vibration, and C–H bending vibration at 1300–650  $\text{cm}^{-1}$  (Huang et al., 2008; Müller et al., 2009; Yao et al., 2010). The absorption peaks of cellulose (2948  $\text{cm}^{-1}$ ), hemicellulose (1730  $\text{cm}^{-1}$ ), and lignin (1739  $\text{cm}^{-1}$ , 1611  $\text{cm}^{-1}$ , 1501  $\text{cm}^{-1}$ , and 812  $\text{cm}^{-1}$ ) in the chemical composition of sandalwood were slightly weakened, indicating that part of it underwent hydrolysis (Honyet al., 2000; Wen et al., 2014). From the FTIR analysis, it was determined that the main chemical components of *Pterocarpus santalinus* extracts are phenols, alcohols, ethers, fatty acids, ketones, polysaccharides, and fatty acids (Fig. 2).

### 3.2. Analysis of TGA and DTG

Fig. 3, presents the thermogravimetric (TG) and derivative thermogravimetric (DTG) curves. From the figure, the changes in mass loss rate of the samples can be elucidated.  $T_{1\text{wt}\%}$ ,  $T_{5\text{wt}\%}$  and  $T_{10\text{wt}\%}$  for weight loss of 1 wt%, 5 wt% and 10 wt%, respectively (Mathi et al., 2016).  $T_{1\text{wt}\%}$ ,  $T_{5\text{wt}\%}$  and  $T_{10\text{wt}\%}$  are 34 °C, 75 °C and 224 °C, respectively. TGA is divided into two stages: water evaporates mainly at low temperature, while the other is the high temperature phase of coke through aerobic combustion. Between 50 and 250 °C, *Pterocarpus santalinus* thermo-gravimetric is only approximately

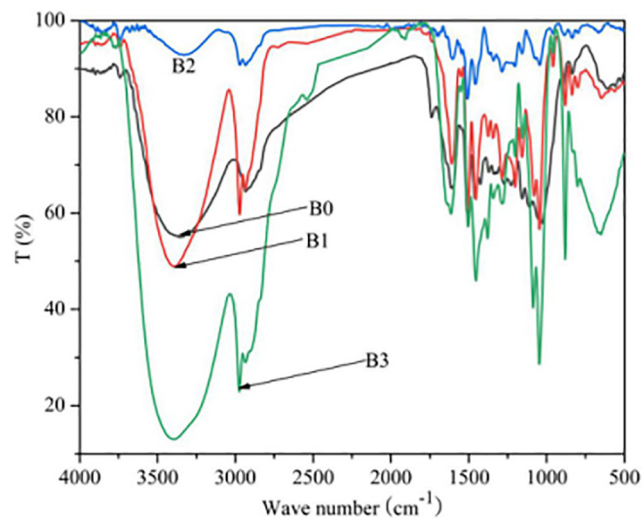


Fig. 1. FT-IR spectra of samples B0, B1, B2, and B3.

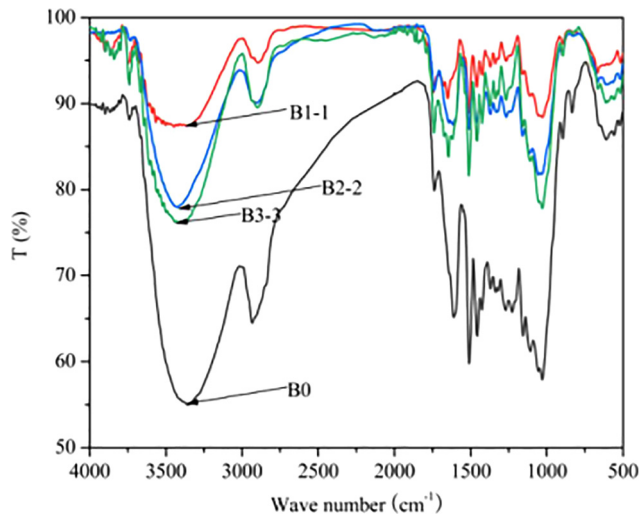


Fig. 2. FT-IR spectra of samples B0, B1-1, B2-2, and B3-3.

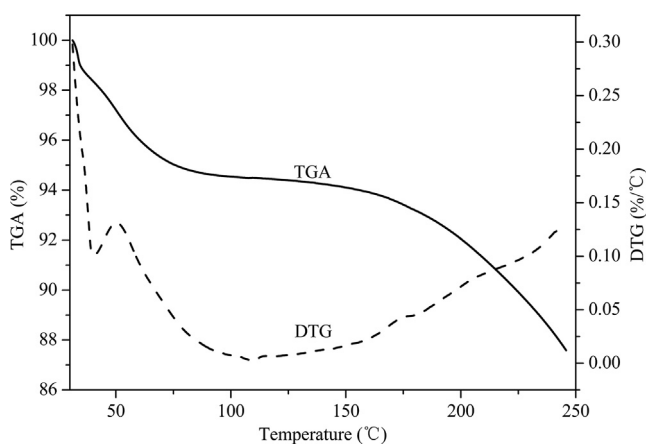


Fig. 3. TGA and DTG thermal curves of *Pterocarpus santalinus*.

13% and thermal weightlessness is less, this phenomenon shows that *Pterocarpus santalinus* thermal stability is better. Moreover, the TGA and DTG tests showed that at 250 °C below, only a small amount of hemicellulose, cellulose and lignin pyrolysis was found in *Pterocarpus santalinus*, showing good thermal stability. Overall, *Pterocarpus santalinus* has better thermal stability.

### 3.3. Analysis of GC-MS

The total ion chromatograms and component distribution obtained from GC-MS analysis of the AB wood waste in the form of extracts are shown in Figs. 4–6.

There is a total of 56 chemical components being identified from the 76 peaks generated by GC-MS analysis of B1 extracts. The results show that the content of more substances are as follows: 2-Naphthalenemethanol, 2-Naphthalenemethanol, decahydro- $\alpha,\alpha,4a$ -trimethyl-8-methylene-, [2R-(2.alpha.,4a.alpha.,8a.beta.)]- (23.7%),  $\alpha$ -Bisabolol (11.32%), Alloaromadendrene oxide-(1) (5.51%), 2-Propen-1-ol, 3-(2,6,6-trimethyl-1-cyclohexen-1-yl)- (13.44%), Estra-1,3,5(10)-trien-17 $\beta$ -ol (5.3%), *cis*-Z- $\alpha$ -Bisabolene epoxide (6.78%), *cis*-Z- $\alpha$ -Bisabolene epoxide (45.01%), 1-Heptatriacotanol (6.08%), 9,12-Octadecadienoic acid (Z,Z)- (5.08%), Oleic Acid (5.36%), 9-Octadecenamamide, (Z)- (6.81%), Heptacosane (10.67%), and Squalene (10.5%). The results show that 56 chemical components being iden-

tified from the 76 peaks generated by GC-MS analysis of B2 extracts. The show that the content of more substances are as follows:  $\alpha$ -Bisabolol (14.18%), Alloaromadendrene oxide-(1) (6.81%), (1R,4aR,7R,8aR)-7-(2-Hydroxypropan-2-yl)-1,4a-dimethyl decahydronaphthalen-1-ol (6.01%), Isospathulenol (11.23%), 2-Propen-1-ol, 3-(2,6,6-trimethyl-1-cyclohexen-1-yl)- (15.04%), 2,4-Dimethyl-5,6-dimethoxy-8-aminoquinoline (10.45%), Isoaromadendrene epoxide (8.81%), *cis*-Z- $\alpha$ -Bisabolene epoxide (50.02%), 2H-1-benzopyran-2-one, and 7-hydroxy-3-(4-methoxyphenyl)- (21.69%). The results show that 57 chemical constituents were identified in B3. The content of more substances are as follows: 2-Naphthalenemethanol, 1,2,3,4,4a,5,6,7-octahydro- $\alpha,\alpha,\alpha,4a,8$ -tetramethyl-, (2R-*cis*)- (7.18%),  $\alpha$ -Bisabolol (14.71%), Alloaromadendrene oxide-(1) (7.3%), (1R,4aR,7R,8aR)-7-(2-Hydroxypropan-2-yl)-1,4a-dimethyldecahydronaphthalen-1-ol (6.62%), (-)-Spathulenol (100%), Isospathulenol (10.53%), 2-Propen-1-ol, 3-(2,6,6-trimethyl-1-cyclohexen-1-yl)- (15.54%), 2,4-Dimethyl-5,6-dimethoxy-8-aminoquinoline (9.02%), *cis*-Z- $\alpha$ -Bisabolene epoxide (8.15%), Ledene oxide-(I) (22.5%), and 10,11-Dihydro-10-hydroxy-2,3,6-trimethoxydibenz(b,f)oxepin (5.23%) (Fig. 7).

### 3.4. Analysis of TDS-GC-MS

According to the results of TDS-GC-MS analysis, 48 chemical constituents were identified in 58 peaks of *Pterocarpus santalinus* volatiles. The results show that the components are: Naphthalene, 1,2,4a,5,8,8a-hexahydro-4,7-dimethyl-1-(1-methylethyl)-, (1.alpha.,4a.beta.,8a.alpha.)-(+/-)- (18.26%), 2-((2R,4aR,8aS)-4a-Methyl-8-methylenedecahydronaphthalen-2-yl)prop-2-en-1-ol (11.48%), Benzene, 1,2,3-trimethoxy-5-(2-propenyl)- (40.97%), *cis*-Z- $\alpha$ -Bisabolene epoxide (11.25%), 2-Naphthalenemethanol,  $\alpha$ -Bisabolol (60.04%), 6-Isopropenyl-4,8a-dimethyl-1,2,3,5,6,7,8,8a-octahydro-naphthalen-2-ol (27.31%), 2-((2R,4aR,8aS)-4a-Methyl-8-methylenedecahydronaphthalen-2-yl)prop-2-en-1-ol (12.42%), 6-Isopropenyl-4,8a-dimethyl-1,2,3,5,6,7,8,8a-octahydro-naphthalen-2-ol (24.85%), and 4-(2,2,6-Trimethyl-7-oxabicyclo[4.1.0]hept-4-en-1-yl)pent-3-en-2-one (11.43%) (Fig. 8).

### 3.5. Analysis of Py-GC-MS

The results of Py-GC-MS show that 50 compounds were identified in *Pterocarpus santalinus*, and the peak area accounted for 47.54% of the total peak area, of which the content was higher: Carbamic acid, monoammonium salt (5.14%), Acetone (3.52%), Glycolaldehyde dimer (5.03%), Acetic acid (3.92%), Phenol, 2-methoxy- (5.02%), Creosol (5.35%), m-Guaiacol (5.77%), 2-Methoxy-4-vinylphenol (5.87%), Phenol, 2,6-dimethoxy- (3.65%), and *trans*-Isoeugenol (3.76%).

### 3.6. Analysis of function

*Pterocarpus santalinus* is a high-end, expensive furniture material. *Pterocarpus santalinus* and *Pterocarpus santalinus* products have a certain human health function. The Py-GC-MS, TDS-GC-MS, and GC-MS techniques were used to analyze the *Pterocarpus santalinus*, obtaining the related compounds. Through literature analysis found that the  $\alpha$ -Bisabolol has anti-inflammatory, antispasmodic, and antiulcer effects, though it also has increased skin defense ability and reduce skin tension. Furthermore, the  $\alpha$ -Bisabolol can efficiently inhibit the human dendritic cell pro-inflammatory activity (Marongiu et al., 2014). Squalene can inhibit the body to absorb cholesterol, which has the function of lowering cholesterol (Smeriglio et al., 2016).

Moreover, the cedrol is a sesquiterpene compound, which is an important component of wood flavor and sandalwood. Not only

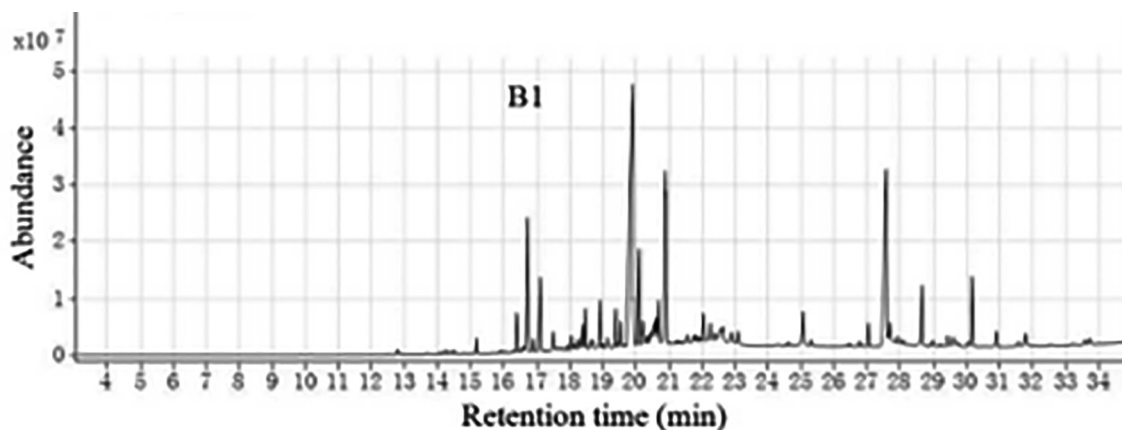


Fig. 4. Total ion chromatograms of *Pterocarpus santalinus* which were extracted by ethanol.

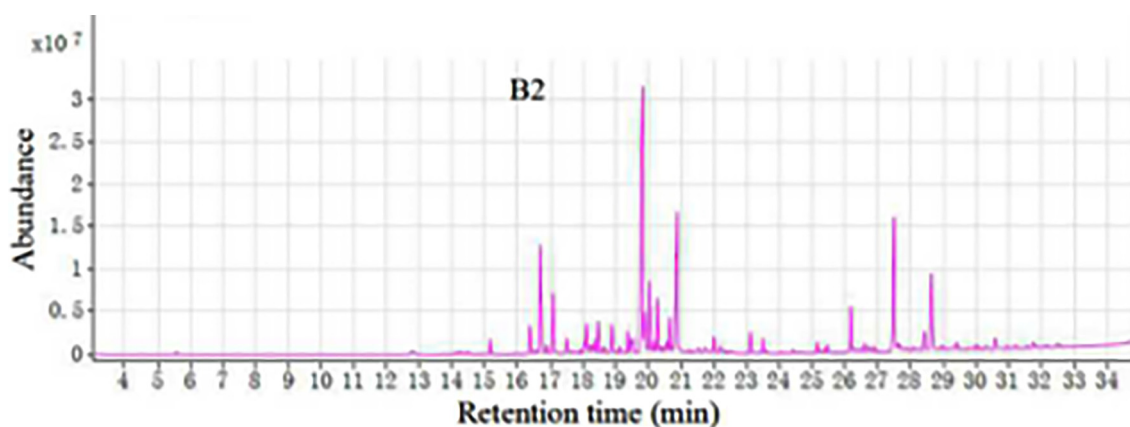


Fig. 5. Total ion chromatograms of *Pterocarpus santalinus* which were extracted by ethanol/benzene (1:2).

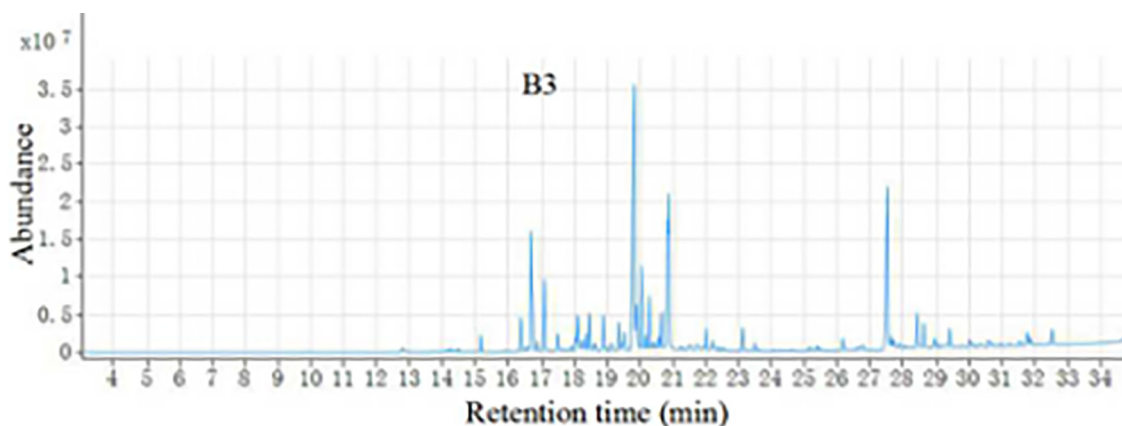


Fig. 6. Total ion chromatograms of *Pterocarpus santalinus* which were extracted by ethanol/benzene (1:1).

that, but it can also be used as a disinfectant, which has the effect of inhibiting human lung cancer cells (Dayawansa et al., 2003). To continue, (-)- Spathulenol has an immune effect (Ziaei et al., 2011). Heptacosane is key in banana leaf volatile oil. *Pterocarpus santalinus* mainly contains unsaturated fatty acids, phytosterols, and polyphenols, which can be used as an antioxidant, anti-aging, lowering blood pressure, improving memory, and other effects. In general, most of the ingredients of sandalwood are healthy and rich, indicating that it contains natural healthy ingredients in terms of health and is a treasure of human health care.

#### 4. Conclusion

In the TG, FTIR, TDS-GC-MS, Py-GC-MS, and GC-MS test, 117 active ingredients were identified in *Pterocarpus santalinus* extract. The main chemical components of *Pterocarpus santalinus* extracts are phenols, alcohols, ethers, ketones, polysaccharides and fatty acids, some of which can be used in high-end perfumes, cosmetics, food and biomedical products. It can be observed from the above studies that the effective components in *Pterocarpus santalinus* are antibacterial, antitumor, and insecticidal activity, of which

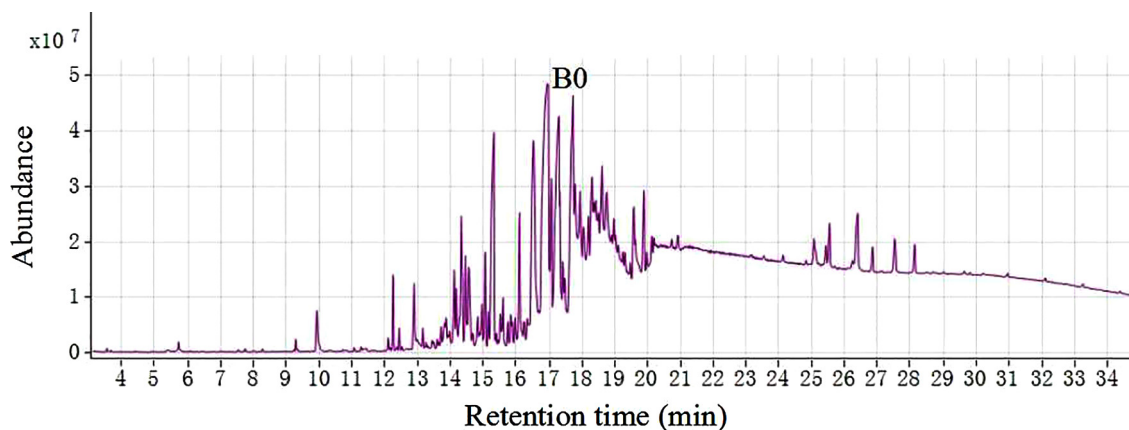


Fig. 7. Total ion chromatograms of *Pterocarpus santalinus* by TDS-GC-MS.

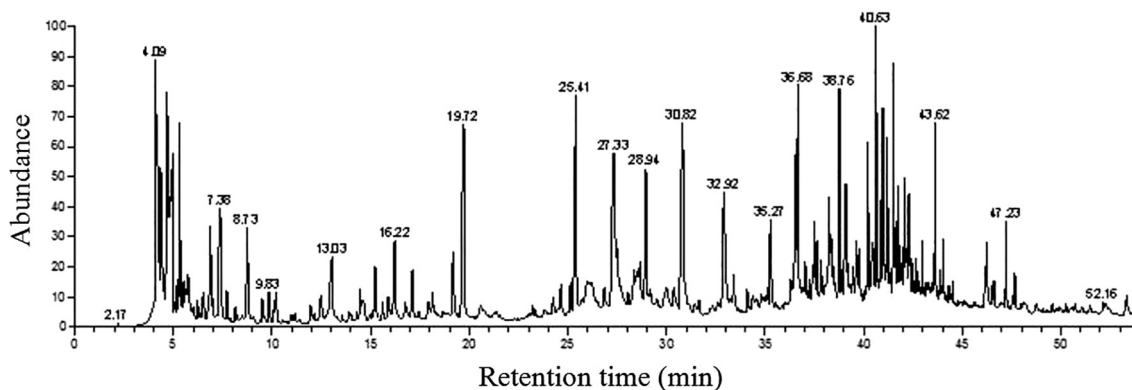


Fig. 8. Total ion chromatograms of *Pterocarpus santalinus* by Py-GC-MS.

the .alpha.-Bisabolol has anti-inflammatory, antispasmodic, and antiulcer effects, while also having increased skin defense ability and reduced skin tension. Squalene can inhibit the body to absorb cholesterol, ultimately lowering cholesterol. The cedrol is a sesquiterpene compound, which is an important component of wood flavor and sandalwood. It can also be used as a disinfectant, which has the effect of inhibiting human lung cancer cells, indicating that it contains natural healthy ingredients in terms of health and is a treasure of human health care.

#### Declaration of Competing Interest

The authors declare that they have no known competing financial interests or personal relationships that could have appeared to influence the work reported in this paper.

#### Acknowledgments

This research was supported by the Planned Science and Technology Project of Hunan Province, China (No.2016SK2089; No.2016RS2011), Major scientific and technological achievements transformation projects of strategic emerging industries in Hunan Province (2016GK4045), Academician reserve personnel training plan of lift engineering technical personnel of Hunan Science and Technology Association (2017TJ-Y10). Yanqiang Wei's contribution as same as the first author, he was also co-first author.

#### References

- Anuradha, M., Pullaiah, T., 1999. Propagation studies of red sanders (*Pterocarpus santalinus* L. f.) in vitro—an endangered taxon of Andhra Pradesh, India. *Taiwania* 44 (3), 311–324.
- Arias, M.E., Polvillo, O., Rodríguez, J., Hernández, M., González-Pérez, J.A., González-Vila, F.J., 2012. Thermal transformations of pine wood components under pyrolysis/gas chromatography/mass spectrometry conditions. *J. Anal. Appl. Pyroly.* 77 (1), 63–67.
- Aydemir, D., Gunduz, G., Altuntas, E., Ertas, M., 2011. Investigating changes in the chemical constituents and dimensional stability of heat-treated hornbeam and uludag fir wood. *Bioresources* 6 (2), 1308–1321.
- Balaban, M., 2004. Identification of the main phenolic compounds in wood of *Ceratonia siliqua* by GC-MS. *Phytochem. Anal.* 15 (6), 385.
- Dayawansa, S., Umeno, K., Takakura, H., Hori, E., Tabuchi, E., Nagashima, Y., Oosu, H., Yada, Y., Suzuki, T., Ono, T., Nishijo, H., 2003. Autonomic responses during inhalation of natural fragrance of cedrol in humans. *Auton. Neurosci. Basic* 108 (1–2), 79.
- Endo, K., Obataya, E., Zeniya, N., Matsuo, M., 2016. Effects of heating humidity on the physical properties of hydrothermally treated spruce wood. *Wood Sci. Technol.* 50 (6), 1161–1179.
- Esteves, B.M., Pereira, H.M., 2009. Wood modification by heat treatment: a review. *Bioresources* 4 (1), 370–404.
- Esteves, B., Graça, J., Pereira, H., 2008. Extractive composition and summative chemical analysis of thermally treated eucalypt wood. *Holzforchung* 62 (3), 344–351.
- Fidêncio, P.H., 2011. Evaluation of chemical composition of eucalyptus wood extracts after different storage times using principal component analysis. *J. Wood Chem. Technol.* 31 (1), 26–41.
- Hony, S., Kerckhoven, C.V., Peeters, E., Tielens, A.G.G.M., Allamandola, L.J., Hudgins, D.M., 2000. The C-H out-of-plane bending modes of PAH molecules in astrophysical environments. *Iso Beyond the Peaks* 370 (3), 1030–1043.

- Huang, A., Zhou, Q., Liu, J., Fei, B., Sun, S., 2008. Distinction of three wood species by Fourier transform infrared spectroscopy and two-dimensional correlation IR spectroscopy. *J. Mol. Struct.* 883–884 (1), 160–166.
- Huang, Y., Wang, Z., Wang, L., Chao, Y., Akiyama, T., Yokoyama, T., Matsumoto, Y., 2016. Analysis of lignin aromatic structure in wood fractions based on IR spectroscopy. *J. Wood Chem. Technol.* 36 (5), 1–6.
- Jiang, S.C., Ge, S.B., Wu, X., Yang, Y.M., Chen, J.T., Peng, W.X., 2017. Treating n-butane by activated carbon and metal oxides. *Toxicol. Environ. Chem.*, 1–12.
- Manjunatha, B., 2006. Antibacterial activity of pterocarpus santalinus. *Indian J. Pharm. Sci.* 68 (1), 115–116.
- Marongiu, L., Donini, M., Bovi, M., Perduca, M., Vivian, F., Romeo, A., Mariotto, S., Monaco, H.L., Dusi, S., 2014. The inclusion into pglg nanoparticles enables  $\alpha$ -bisabolol to efficiently inhibit the human dendritic cell pro-inflammatory activity. *J. Nanopart. Res.* 16 (8), 1–16.
- Mathi, P., Veeramachaneni, G.K., Raj, K.K., Talluri, V.R., Bokka, V.R., Botlagunta, M., 2016. In vitro and in silico characterization of angiogenic inhibitors from sophora interrupta. *J. Mol. Model.* 22 (10), 247.
- Mi, C., Wang, J., Mi, W., et al., 2019. Research on regional clustering and two-stage SVM method for container truck recognition. *Discrete Continuous Dyn. Syst. Ser. S* 12 (4–5), 1117–1133.
- Mohareb, A., Sirmah, P., Pétrissans, M., Gérardin, P., 2012. Effect of heat treatment intensity on wood chemical composition and decay durability of pinus patula. *Eur. J. Wood Wood Prod.* 70 (4), 519–524.
- Müller, G., Schöpfer, C., Vos, H., Kharazipou, A., Polle, A., 2009. FTIR-ATR spectroscopic analysis of changes in wood properties during particle- and fibreboard production of hard- and softwood trees. *Bioresources* 4 (1), 49–71.
- Peng, W., Maleki, A., Rosen, M.A., et al., 2018. Optimization of a hybrid system for solar-wind-based water desalination by reverse osmosis: comparison of approaches. *Desalination* 442, 16–31.
- Peng, W.X., Wang, L.S., Xu, Q., Wu, Q.D., Xiang, S.L., 2012. TD-GC-MS analysis on thermal release behavior of poplar composite biomaterial under high temperature. *J. Comput. Theor. Nanos.* 9 (9), 1431–1433.
- Peng, W.X., Xue, Q., Ohkoshi, M., 2014. Immune effects of extractives on bamboo biomass self-plasticization. *Pak. J. Pharm. Sci.* 27 (4 Suppl), 991–999.
- Shen, Y., Zhao, N., Xia, M., et al., 2017. A deep Q-learning network for ship stowage planning problem. *Polish Marit. Res.* 24 (SI), 102–109.
- Smeriglio, A., Galati, E.M., Monforte, M.T., Lanuzza, F., D'Angelo, V., Circosta, C., 2016. Polyphenolic compounds and antioxidant activity of cold-pressed seed oil from finola cultivar of cannabis sativa l. *Phytotherapy Res.* 30 (8), 1298.
- Tumen, I., Aydemir, D., Gunduz, G., Uner, B., CetiN, H., 2010. Changes in the chemical structure of thermally treated wood. *Bioresources* 5 (3), 1936–1944.
- Wang, S., Ru, B., Lin, H., Sun, W., Luo, Z., 2015. Pyrolysis behaviors of four lignin polymers isolated from the same pine wood. *Bioresource Technol.* 182, 120–127.
- Wen, J.L., Sun, S.L., Yuan, T.Q., Xu, F., Sun, R.C., 2014. Understanding the chemical and structural transformations of lignin macromolecule during torrefaction. *Appl. Energy* 121 (10), 1–9.
- Xue, Q., Peng, W.X., Ohkoshi, M., 2014. Molecular bonding characteristics of self-plasticized bamboo composites. *Pak. J. Pharm. Sci.* 27 (4 Suppl), 975.
- Yao, X., Peng, Y., Zhou, Q., Xiao, P., Sun, S., 2010. Distinction of eight lycium, species by Fourier-transform infrared spectroscopy and two-dimensional correlation IR spectroscopy. *J. Mol. Struct.* 974(1–3) 161–164.